Article

Not peer-reviewed version

Comparison of the Diagnostic Value of Mono-Exponential, Bi-Exponential, and Stretched Exponential Diffusion-Weighted MRI to Predict Hepatic Lymph Node Metastases in Patients with Colorectal Liver Metastases after Chemotherapy

Hai-Bin Zhu , Bo Zhao , Xiao-Ting Li , Xiao-Yan Zhang , Qian Yao , Ying-Shi Sun *

Posted Date: 19 September 2023

doi: 10.20944/preprints202309.1264.v1

Keywords: colorectal cancer; individualized treatment; diffusion magnetic resonance imaging; intravoxel incoherent motion; liver

Article

Comparison of the Diagnostic Value of Mono-Exponential, Bi-Exponential, and Stretched Exponential Diffusion-Weighted MRI to Predict Hepatic Lymph Node Metastases in Patients with Colorectal Liver Metastases after Chemotherapy

Hai-bin Zhu [1,†], Bo Zhao [1,†], Xiao-Ting Li [1], Xiao-Yan Zhang [1], Qian Yao [2] and Ying-Shi Sun [1,*]

[1] Key Laboratory of Carcinogenesis and Translational Research (Ministry of Education/Beijing), Department of Radiology, Peking University Cancer Hospital & Institute, 52 Fu Cheng Road, Hai Dian District, Beijing 100142, China; 13811403328@163.com (H-b.Z.); zhaobur123@163.com (B.Z.); 13520120308@163.com (X-T.L.); 370493077@qq.com (X-Y.Z.)

[2] Key Laboratory of Carcinogenesis and Translational Research (Ministry of Education), Department of Pathology, Peking University Cancer Hospital & Institute, Hai Dian District, Beijing 100142, China; yaoqian@aliyun.com (Q.Y.)

* Correspondence: sys27@163.com

† Hai-bin Zhu and Bo Zhao contributed equally to this work.

Simple Summary: In this study, we compared the diagnostic efficacy of mono-exponential, bi-exponential, and stretched exponential Diffusion-weighted MRI in predicting hepatic lymph node metastases in patients with colorectal liver metastases after chemotherapy. Our results revealed that only pre- treatment DDC value and the short diameter of the largest lymph node after treatment were independent predictors of hepatic lymph nodes metastases. We constructed a nomogram incorporating these two factors to predict the status of hepatic lymph nodes non-invasively and individually, which showed great potential in surgical planning and high-risk patients' assessment.

Abstract: Colorectal liver metastases (CRLM) patients combined with hepatic lymph node metastases was a negative prognostic factor associated with outcomes. Up to now, there was still lack of a reliable method to identify the status of hepatic lymph nodes. The aim of this study was to investigate the predictive ability of mono-exponential, bi-exponential, and stretched-exponential diffusion-weighted imaging (DWI) models to distinguish between benign and malignant hepatic lymph nodes in CRLM patients who underwent neoadjuvant chemotherapy prior to surgery. In total, 97 CRLM patients with pathologically proved hepatic lymph node status were included. Various quantitative parameters, including the apparent diffusion coefficient (ADC) from mono-exponential model, D, D*, and f derived from intravoxel incoherent motion (IVIM) model, as well as DDC and α from stretched-exponential model (SEM), were measured. Multivariate analysis revealed that the pre- treatment DDC value and the short diameter of the largest lymph node after treatment were independent predictors of metastatic hepatic lymph nodes. A nomogram combining these two factors demonstrated excellent performance in distinguishing between benign and malignant lymph nodes in CRLM patients, with an area under the curve (AUC) of 0.873. Therefore, the nomogram can serve as a preoperative assessment tool for determining the status of hepatic lymph nodes and aiding in the decision-making process for surgical treatment in CRLM patients.

Keywords: colorectal cancer; individualized treatment; diffusion magnetic resonance imaging; intravoxel incoherent motion; liver

INTRODUCTION

Colorectal carcinoma is the most common digestive tumors in the world and more than 50% patients would develop colorectal liver metastases (CRLM) at diagnosis (synchronous metastases) or

 doi:10.20944/preprints202309.1264.v1

during the follow-up (metachronous metastases) [1]. Currently, perioperative chemotherapy in combination with surgical resection, whenever a complete resection with adequate residual liver parenchyma is feasible, is the first choice in the standard treatment guidelines [2,3]. About 10-31% CRLM patients would have hepatic lymph node metastases (LNM), which was a negative prognostic factor associated with outcomes [4,5]. Surgery remains the only potentially curative therapy if LNM are confined to the hepatic pedicle, although this procedure can be linked with potential postoperative complications such as bleeding, lymphatic leakage and ischemic bile duct stricture [6,7].

The golden standard for judging LNM is still determined by histopathological assessment after operation. To date, indications for lymphadenectomy in CRLM are not consistent partly due to the challenge of preoperatively prediction of LNM. For example, Grobmeyer et al. [8] exanimated 100 patients with hepatic lymph nodes undergoing resection for primary and metastatic hepatic malignancies. They found that both CT and intraoperative clinical assessment by palpation had a high negative predictive value (NPV= 95% and 99 %, respectively) with a low positive predictive value (PPV= 30% and 39 %, respectively). Similarly, Rau et al. [9] found that the short diameter of lymph node larger than 15 mm and a morphologically round shape on CT had a high negative predictive value (NPV) of 85% but a relatively low positive predictive value (PPV) of 43% for LNM. In addition, interestingly, up to 27% of the patients with confirmed pathological LNM were not initially suspected using in combination of CT and intraoperative examination. Therefore, reliable predictors of LNM in CRLM before surgery are needed for guiding accurately individual decision-making and avoiding overtreatment in low-risk patients.

Diffusion-weighted magnetic resonance imaging (DWI) has been extensively studied for its applications in cancer detection, treatment response assessment, and prognosis evaluation [10–12]. Apparent diffusion coefficient (ADC), calculated from DWI, has shown great potential in lymph node differentiation due to it can noninvasively assess the microscopic random Brownian motion of water molecules in biological tissues. For instance, Sumi et al. [13] found higher ADC values in metastatic lymph nodes compared to benign non-metastatic lymph nodes, while Razek et al. [14] and Eiber et al. [15] showed a totally different conclusion that lower ADC values in metastatic lymph nodes. This discrepancy may be attributed to the fact that ADC values are calculated using a mono-exponential decay formula, which assumes tissue homogeneity and the movement of water molecules with a Gaussian distribution. Intravoxel incoherent motion (IVIM) is a technique that can potentially separate the perfusion components from the pure diffusion of water molecules using a biexponential model. This model allows for the quantification of three parameters: the true diffusion coefficient (D), the pseudo-diffusion coefficient (D*), and the perfusion fraction (f). Therefore, parameters obtained from IVIM model have demonstrated better diagnostic performance than traditional ADC in the differentiating of hepatic lesions in previous studies [17]. More recently, Bennett et al. [18] introduced the stretched-exponential model (SEM), which offers an alternative approach to quantify intravoxel heterogeneity. The SEM utilizes two parameters: the distributed diffusion coefficient (DDC) and the intravoxel water diffusion heterogeneity (α). However, to date, there is still a lack of studies comparing functional MRI parameters calculated from different models to determine the status of hepatic lymph nodes in CRLM patients.

The aim of this study was to evaluate the diagnostic accuracy of three mathematical models of DWI in differentiating between benign and malignant hepatic lymph nodes in CRLM patients who underwent chemotherapy prior to surgery.

MATERIALS AND METHODS

Study participants

This retrospective study protocol was approved by the Medical Ethics Committee of Beijing Cancer Hospital(Approval Number 2023KT83), and informed consent was waived.

CRLM patients with pathologic diagnosis of hepatic lymph nodes in our hospital between January 2015 and January 2023 were retrieved in this study. Patients should receive at least two cycles

 doi:10.20944/preprints202309.1264.v1

of neoadjuvant chemotherapy and undergo MRI examinations before neoadjuvant chemotherapy (pre-treatment point) and within 1 month before surgery (post-treatment point). The exclusion criteria were: 1) patients who underwent hepatectomy without hepatic lymph node resection; 2) patients without measurable hepatic lymph node >5 mm on the baseline MRI; 3) patients without multiple b-values of DWI sequence or the quality of DWI was not sufficient for analysis. Totally, 97 patients were enrolled in this study.

MRI protocol

All patients in this study underwent MRI examinations using a 1.5T MRI device (Signa Excite II; GE Healthcare, Milwaukee, WI, USA) equipped with an 8-channel phased array body coil. The imaging protocol consisted of several sequences, including: axial T2-weighted imaging (T2WI) with fat saturation, multiple b-values of DWI, and dynamic contrast-enhanced (DCE) MRI sequences. Respiratory-triggered single-shot echo planar imaging sequence was used for DWI, with the b-values of 0, 20, 50, 100, 200, 600, 800, 1000, 1200, and 1500 s/mm^2, respectively. The DWI sequence parameters were as follows: repetition time (TR)/ echo time (TE) = 3000/80; slice thickness = 6 mm; slice gap = 1 mm; matrix = 128 x 90. The total acquisition time for the DWI sequence was approximately 6 minutes and 19 seconds. The corresponding parameters for the T2WI were: TR/TE = 12,630/70 ms; slice thickness = 6 mm; slice gap = 1 mm; matrix = 228 x 224.

MRI Image Analysis

Images were analyzed independently by two radiologists (B.Z., with 6 years of experience, and H.B.Z with 12 years of experience), using the FuncTool Software implemented in GE Workstation 4.6. The two radiologists were blinded to clinical information, pathological results and each other's results. To determine the regions of interest (ROI), the radiologists manually drew the ROI on the DWI image with a b-value of 800 s/mm^2 at the maximum transverse diameter of the hepatic lymph node, while avoiding areas containing adjacent vessels and artifacts. T2WI and DCE-MRI images were used as references. Furthermore, the mean value of parameters obtained from two observers for each ROI was calculated for further analysis.

The signal intensity (SI) of each ROI was fitted using the following mathematical models: where S(b) is SI at a particular b value and S (0) is SI with b = 0 s/mm^2.

1. ADC was calculated using the mono-exponential model:

$$S(b)/S(0) = \exp(-b \times ADC)$$

2. Three parameters were calculated using biexponential IVIM model according to the following equation:

$$S(b)/S(0) = f \times \exp(-b \times D*) + (1-f) \times (-b \times D)$$

D represents the true diffusion coefficient, D* represents pseudo-diffusion coefficient, and f represents the fraction of pseudo-diffusion.

3. DDC and α were acquired from SEM using the following mathematical equation:

$$S(b)/S(0) = \exp\{-(b \times DDC)\}^{\alpha}$$

DDC represents the distributed diffusion coefficient, which characterizes the distribution of diffusion rates within a voxel. α, ranging from 0 to 1, represents intravoxel diffusion heterogeneity.

Surgical technique and Clinical information

The hepatic lymph nodes were defined based on specific criteria. These criteria included nodes located along the hepatoduodenal ligament, which encompasses structures such as the proper hepatic artery, portal vein, bile duct, and retro-pancreatic head. Additionally, nodes located along the common hepatic artery and coeliac artery were also included, which includes the coeliac, common hepatic, and left gastric arteries. As hepatic lymph nodes were not routinely dissected, only suspected

 doi:10.20944/preprints202309.1264.v1

hepatic lymph nodes on preoperative imaging and/or intro-operation examination were removed. The hematoxylin and eosin (H&E) stained specimens of the surgically removed lymph nodes were evaluated by specialized pathologists. All pathological results were obtained according to the final pathological reports.

Clinical information of CRLM patients was also collected retrospectively, including age, sex, location (left half colon vs right half colon), T and N stage of the primary tumor, synchronous liver metastases or metachronous liver metastases, number of liver metastases (single vs multiple), RAS gene status (mutation type vs wild type), treatment response based on RECIST1.1 standard, disappearing lesions, carcinoembryonic antigen (CEA) and carbohydrate antigen 19-9 (CA19-9) level. Disappearing lesions after chemotherapy can only be identified when no visible lesion is observed on all imaging sequences. Serum tumor markers were categorized into two groups based on their levels: those within normal limits and those higher than normal limits. The normal limits for CEA and CA19-9 were defined as 5 ng/mL and 40 ng/mL, respectively.

Statistical analysis

Continuous variables are described as mean ± standard deviation while categorical variables are described as numbers with percentages. To compare characteristics between the two groups, independent-samples t/Mann–Whitney or chi-square tests were used. To determine independent factors associated with hepatic LNM, multivariable logistic regression was performed using a forward stepwise approach. The diagnostic performance of the predictive model was evaluated using the receiver operating characteristic (ROC) curve. The area under the ROC curve (AUC) with its 95% confidence interval was calculated. The cutoffs for the model were determined using the maximum Youden's method. Sensitivity, specificity, positive predictive value (PPV), and negative predictive value (NPV) were also calculated to assess the performance of the model. Inter-observer agreements of quantitative metrics were tested using intraclass correlation coefficients (ICC). ICC > 0.75, 0.40 to 0.75 or ⩽0.40 were considered indicative of good, moderate or poor agreement, respectively. All statistical analyses were conducted using SPSS 25.0 (IBM Corporation, Armonk, NY, USA). A two-sided P value of less than 0.05 was considered statistically significant, indicating a significant difference or association between variables.

Results

Clinicopathologic Characteristics

Among the 97 enrolled patients, 40 patients (41.2%; mean age = 57.53±9.43 years) showed hepatic LNM while the other 57 patients (58. 8%; mean age = 52.91±10.48 years) did not.

Univariate and Multivariate Analyses for Factors associated with hepatic LNM

At univariate analysis, short and long axis of the largest lymph node before treatment, short and long axis of the largest lymph node after treatment, pre-treatment D, pre-treatment DDC, post-treatment ADC, post-treatment DDC and post-treatment α were found to be statistically significant with hepatic LNM ($P < 0.05$).

At multivariate analysis, only pre-treatment DDC (OR, <0.001, P=0.002) and the short axis of the largest lymph node after treatment (OR, 1.509; $P < 0.001$) were the independent risk factors for the status of hepatic LNM. The detailed results of the univariate and multivariate analyses are presented in Table 1.

Preprints (www.preprints.org) | NOT PEER-REVIEWED | Posted: 19 September 2023 doi:10.20944/preprints202309.1264.v1

Table 1. Univariate and multivariate analysis of clinical and MRI factors for prediction of hepatic lymph nodes metastases.

		Univariate analysis			Multivariate Analysis	
		Non-hepatic LNM (n=57)	hepatic LNM HLN(n=40)	P value	OR (95% confidence interval)	P value
Gender	male/female	44/13	27/13	**0.029***		
Age		52.91±10.48	57.53±9.43	0.054		
BMI		24.63±3.04	24.50±3.04	0.842		
Primary location	Right-/left-side	15/42	6/34	0.944		
Differentiation	Low to moderate/High	55/2	40/0	0.510		
T stage of primary tumor	T1+2/T3+4	3/54	4/36	0.650		
N stage of primary tumor	N0/N+	9/48	5/35	0.149		
Gene	RAS-wild/mutation	38/19	28/12	0.729		
Simultaneous liver metastases	No/Yes	13/44	12/28	0.425		
Distribution	Solitary/Bilateral	20/37	15/25	0.808		
Number of CRLM	≤3/＞3	17/40	15/25	0.429		
Size(mm)		38.25±27.69	37.88±22.11	0.944		
RECIST	Response/Non-Response	33/24	21/19	0.599		
Disappearing lesion	No/Yes	46/11	34/6	0.584		
pre-CEA	≤5/＞5ng/ml	15/42	11/29	0.897		
pre-CA199	≤40/＞40U/ml	26/31	17/23	0.761		
post-CEA	≤5/＞5ng/ml	27/30	17/23	0.635		
post-CA199	≤40/＞40U/ml	33/24	25/15	0.649		
Short axis of largest lymph node before treatment	mm	7.39±2.65	11.88±5.35	**＜0.001***		
Long axis of largest lymph node before treatment	mm	14.25±6.41	18.28±7.28	**0.005***		
Pre-ADC	mm^2/s	1.54±0.35	1.49±0.30	0.394		
Pre-D	mm^2/s	1.21±0.43	1.02±0.25	**0.005***		
Pre-D*	mm^2/s	3.33±2.37	2.70±2.38	0.200		
Pre-f		0.49±0.17	0.45±0.14	0.330		
Pre-DDC	mm^2/s	3.21±1.69	2.01±0.83	**＜0.001***	<0.001	**0.002***
Pre-α		0.59±0.17	0.62±0.16	0.363		
Short axis of largest lymph node after treatment	mm	6.74±2.13	10.43±3.62	**＜0.001***	1.509(1.235-1.845)	**＜0.001***
Long axis of largest lymph node after treatment	mm	13.46±5.78	17.08±6.82	**0.006***		
Post-ADC	mm^2/s	1.64±0.32	1.45±0.32	**0.006***		
Post -D	mm^2/s	1.35±0.86	1.24±0.78	0.529		
Post -D*	mm^2/s	3.69±2.96	3.48±3.38	0.751		
Post -f		0.51±0.18	0.52±0.18	0.732		
Post-DDC		3.46±1.48	2.37±0.91	**＜0.001***		
Post -α		0.61±0.13	0.67±0.13	**0.035***		

Note: ADC, Apparent diffusion coefficient; CEA, carcinoembryonic antigen; CA19-9 carbohydrate antigen 19-9; CI: confidence interval; CRLM, colorectal liver metastases; DDC: distributed diffusion coefficient; RECIST, Response Evaluation Criteria In Solid Tumors; *p values that are significantly different between metastatic and non- metastatic HLN group.

Preprints (www.preprints.org) | NOT PEER-REVIEWED | Posted: 19 September 2023 doi:10.20944/preprints202309.1264.v1

Comparison of parameters from models for Prediction hepatic LNM

Table 2 summarizes the results of ROC analysis for quantitative parameters from all three models for prediction hepatic LNM. For the prediction of hepatic LNM, pre-DDC had the largest area under curve (AUC = 0.770; 95% CI = 0.676-0.865), followed by post-DDC (AUC = 0.739; 95% CI = 0.641-0.838) and post-ADC (AUC = 0.664; 95% CI =0.553-0.774). The sensitivity, specificity, PPV, NPV, and accuracy of pre-DDC for differentiating malignant and benign hepatic lymph nodes were 85.0%, 59.6%, 59.6%, 85.0% and 70.1%, respectively, with an optimal cutoff value of 1.92×10^{-3} mm^2/s.

Table 2. Diagnostic performance of quantitative parameters and nomogram in predicting hepatic LNM in CRLM patient.

	AUC	Cut off value	Sensitivity (%)	Specificity (%)	PPV (%)	NPV (%)	Accuracy (%)
Pre-ADC	0.551(0.436-0.666)	1.70	32.5	82.5	56.5	63.5	61.5
Pre-D	0.648(0.538-0.758)	1.15	55.0	77.2	62.9	58.1	68.0
Pre-D*	0.592(0.477-0.707)	2.51	55.0	66.7	53.7	71.0	62.1
Pre-f	0.577(0.462-0.692)	3.98	70.0	47.5	48.3	64.3	56.7
Pre-DDC	0.770(0.676-0.865)	1.92	85.0	59.6	59.6	85.0%	70.1
Pre-α	0.573(0.456-0.689)	0.59	62.5	59.6	52.1	69.4	60.8
Post-ADC	0.664(0.553-0.774)	1.46	75.0	52.6	52.6	75.0	61.9
Post -D	0.581(0.447-0.681)	1.21	50.0	70.2	54.1	66.7	62.1
Post -D*	0.558(0.438-0.678)	1.27	85.0	33.3	47.2	76.0	54.6
Post -f	0.521(0.403-0.638)	3.98	77.5	31.6	44.3	66.7	50.5
Post-DDC	0.739(0.641-0.838)	2.26	82.5	52.5	55.0	81.1	64.9
Post-α	0.623(0.509-0.737)	0.65	57.5	70.2	57.5	70.2	65.0
Short axis of largest lymph node before treatment (mm)	0.773(0.674-0.872)	12	50.0	94.7	87.0	73.0	76.3
Short axis of largest lymph node after treatment (mm)	0.811(0.724-0.899)	10	52.5	94.7	38.9	74.0	77.3
Nomogram	0.873(0.803,0.943)	1.03	82.5	82.5	87.0	76.7	82.5

Note: AUC, Area Under Curve.

In addition, short axis of the largest lymph node before and after treatment also showed good performance in predicting of hepatic LNM. The highest accuracy (77.3%) was achieved at a cutoff value of 10mm (the best cut off value = 9.5mm) for short axis of the largest hepatic lymph node after treatment, which had 52.5% sensitivity and 94.7% specificity for differentiating the status of hepatic lymph nodes.

Development the Nomogram for Prediction hepatic LNM

The nomogram in combination with pre-treatment DDC and the short axis of the largest lymph node after treatment demonstrated good performance in predicting hepatic LNM. The AUC of the nomogram was 0.873(95% CI = 0.803-0.943) (Figure 1), with sensitivity, specificity, PPV, NPV, and accuracy were 82.5%, 82.5%, 87.0%, 76.7% and 82.5%, respectively. The nomogram for prediction hepatic LNM is presented in Figure 2.

Preprints (www.preprints.org) | NOT PEER-REVIEWED | Posted: 19 September 2023 doi:10.20944/preprints202309.1264.v1

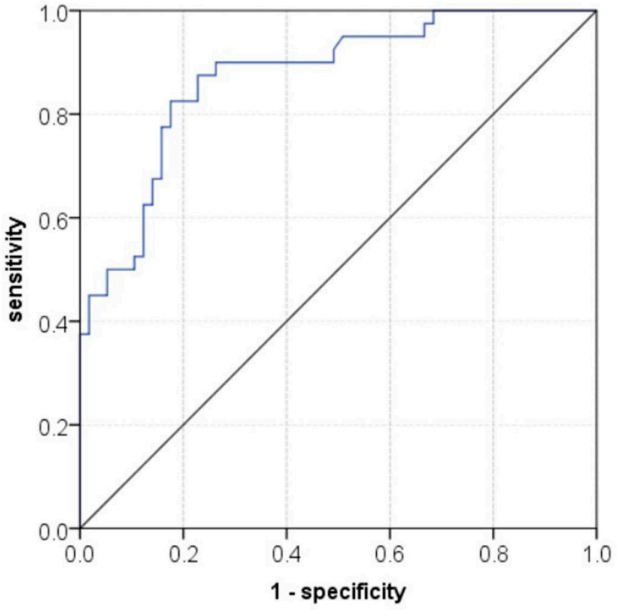

Figure 1. Receiver operating characteristics curves of nomogram to predict hepatic LNM in CRLM patients receiving chemotherapy.

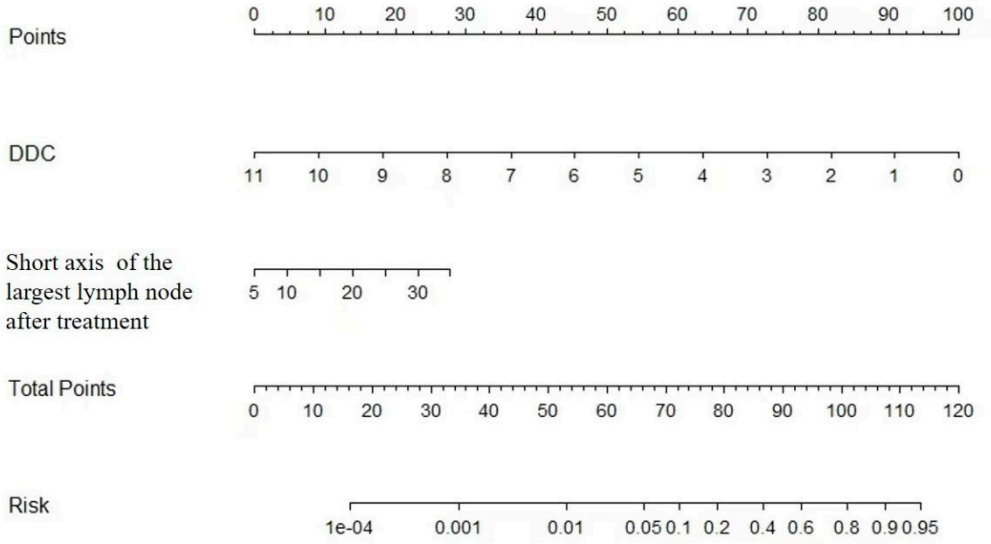

Figure 2. Nomogram of model for predicting hepatic LNM in CRLM patients receiving chemotherapy.

Interobserver Agreement for Radiologic Parameters

Moderate or good inter-observer agreement were obtained for quantitative parameters (ICC range: 0.47–0.83). The ICCs of DDC before and after treatment were 0.52 and 0.81, respectively.

Discussion

In this study, we assessed the diagnostic potential of DWI parameters using three models to distinguish between benign hepatic lymph nodes and metastatic lymph nodes in initially resectable CRLM patients. Our findings demonstrate that the values of DDC obtained from the stretched-exponential model were significantly lower in metastatic lymph nodes compared to non-metastatic lymph nodes, both before and after treatment. Furthermore, we found that the DDC value at baseline exhibited the highest accuracy for preoperative diagnosis of lymph node status in CRLM patients,

 doi:10.20944/preprints202309.1264.v1

surpassing the accuracy of ADC from the mono-exponential model, as well as D, D*, and f from the IVIM model. Additionally, there was substantial agreement between two independent readers in assessing DDC, suggesting that DDC, in combination with the short diameter of the largest lymph node, may serve as a reliable, non-invasive and promising technique in clinical practice for differentiating between metastatic and non-metastatic lymph nodes prior to surgery.

Our results found that the baseline DDC from the SEM exhibited the highest diagnostic performance in distinguishing metastatic from benign hepatic lymph nodes, followed by post-DDC and post-ADC, although the differences among them were not significant. DDC value was considered as a weighted sum of continuous distributions of ADCs and can provide more information on non-Gaussian distribution. Our results can be explained by increased cellularity, higher nucleus-to-cytoplasm ratios and more limited extracellular space in malignant lymph node, which can lead to more intravoxel diffusion heterogeneity [19,20]. Consequently, DDC may possess the greatest capability to differentiate between benign and malignant liver lesions with minimal overlap in comparison with ADC calculated from mono-exponential model, which were in consistent with previous studies on gliomas, ovarian cancer, bladder cancer and hepatic lesions [21–24]. Meanwhile, DDC values calculated from SEM was more reliable than the mono-exponential and IVIM model, which was in alliance with previous studies [25–27].

Conversely, although the quantitative parameters obtained from IVIM model, with the exception of post-f of benign hepatic lesions, were higher in malignant lymph nodes, the difference was not statistically significant. Several factors may contribute to these results. First, the value of the IVIM model in predicting lymph nodes status was not completely consistent in previous literature. For example, Jia et al. [28] conducted a study on rectal adenocarcinoma patients and found that the group with positive lymph nodes exhibited a significantly lower D* value and a higher f value. However, in another study on rectal cancer patients, the metastatic group exhibited significantly lower D and D* values compared to the nonmetastatic group [29]. Too many factors may influence the results of IVIM parameters, such as the setting of b-values (especially b-values < 200 s/mm^2), repetition time and scan techniques. Secondly, the heterogeneity of hepatic lesions can also affect the quantitative parameters of the IVIM model. Malignant lesions often exhibit more heterogeneity in terms of cellularity, vascularity, and perfusion compared to benign lesions. This inherent heterogeneity can lead to variations in the IVIM parameters, making it difficult to differentiate between benign and malignant lesions based solely on IVIM parameters. In addition, the limited sample size in our study may also lead to selection bias.

We discovered that short diameter of the largest lymph node after treatment were helpful in predicting the status of hepatic lymph node in CRLM patients. This finding is consistent with that of previous study, which indicated that tumor size was an independent predictor of lymph node metastasis [30]. The optimal diagnostic threshold for short diameter of lymph nodes was 10 mm in our study, with sensitivity, specificity and accuracy were 52.5%, 94.7% and 77.3%, respectively. Nomogram combined with DDC and short diameter of the largest lymph node can be used to quantitatively evaluate lymph node metastasis with better diagnostic efficacy. The diagnostic efficiency of the nomogram, with an AUC of 0.873, demonstrated higher performance compared to using either IVIM or SEM alone. Additionally, the nomogram showed improved sensitivity, specificity, and accuracy. These results suggest that the nomogram can effectively prevent unnecessary lymph node dissection in CRLM patients.

There were several limitations in the present study. First, this was a retrospective, single-center study with a relatively small sample size. Therefore, further studies with a larger sample size and external validation are needed to confirm the findings. Secondly, there may be selection bias because we only enrolled patients with clinically suspected lymph node metastasis who underwent surgical resection. This could potentially underestimate the severity of the condition as most patients with colorectal liver metastasis were excluded if they did not have clinically suspicious metastatic lymph nodes. Thirdly, there may be a lack of certainty regarding the alignment between the lymph node evaluated by the pathologist and the image slices where the DWI parameters were obtained. Additionally, the setting of b-values in DWI still remains controversial. While using too many b-

values would result in prolonged scan time, further research is required to determine the optimal number and interval of b-values for accurate assessment. Lastly, we did not analyze the relationship between models and survival outcome of the patients in this study.

Conclusions

In conclusion, our results indicate that nomogram incorporating pre-DDC value calculated from SEM-DWI along with the short diameter of the largest lymph node after treatment may have potential to predict lymph node metastasis noninvasively in CRLM patients after chemotherapy. This nomogram can be utilized for individualized, noninvasive high-risk assessment and surgical planning of CRLM patients with suspected metastatic hepatic lymph nodes, thereby reducing unnecessary surgical procedures and the occurrence of complications.

Author Contributions: Conception and design: HB.Z., B.Z., YS.S.; Collection and assembly of data: HB.Z., B.Z., Q.Y.; Development of methodology: HB.Z., B.Z., X.Y.Z, XT. L., YS.S.; Data analysis and interpretation: HB.Z., B.Z., XT.L., YS.S.; Manuscript writing: All authors; Final approval of manuscript: All authors.

Funding: This work was supported by Beijing Hospitals Authority Youth Program (QML20231103) and Beijing Hospitals Authority Ascent Plan (Code: 20191103).

Institutional Review Board Statement: This study was approved by the ethical review board committee of Peking University Cancer Hospital and Institute (Beijing, China). All data were anonymized.

Informed Consent Statement: The requirement for informed consent was waived due to its retrospective design.

Data Availability Statement: The data used in this study are available from the corresponding author upon reasonable request.

Conflicts of Interest: The authors declared no conflict of interest.

Abbreviations

ADC	apparent diffusion coefficient
AUC	area under the curve
CI	confidence interval
CRLM	colorectal liver metastases
CT	computed tomography
CV	coefficient of variation
DCE-MRI	dynamic contrast-enhanced magnetic resonance imaging
DDC	distributed diffusion coefficient
DWI	diffusion weighted imaging
FOV	field of view
LNM	lymph node metastases
ICCs	intraclass correlation coefficients
IVIM	intravoxel incoherent motion
MRI	magnetic resonance imaging
NPV	negative predictive value
PPV	positive predictive value
ROC	receiver operating characteristic
ROI	regions of interest
SEM	stretched-exponential model
SI	signal intensity
TE	echo time
TR	repetition time

References

1. Ferlay, J.; Soerjomataram, I.; Dikshit, R.; Eser, S.; Mathers, C.; Rebelo, M.; Parkin, DM.; Forman, D.; Bray, F. Cancer incidence and mortality worldwide: sources, methods and major patterns in GLOBOCAN 2012. Int J Cancer. 2015, 127, E359-86.
2. Nieuwenhuizen, S.; Puijk, RS.; van den Bemd, B.; Aldrighetti, L.; Arntz, M.; van den Boezem, PB.; Bruynzeel, AME.; Burgmans, MC.; de Cobelli, F.; Coolsen, MME.; et al. Resectability and Ablatability Criteria for the Treatment of Liver Only Colorectal Metastases: Multidisciplinary Consensus Document from the COLLISION Trial Group. Cancers (Basel). 2020, 12, 1779.
3. Morris, VK.; Kennedy, EB.; Baxter, NN.; Benson, AB 3rd.; Cercek, A.; Cho, M.; Ciombor, KK.; Cremolini, C.; Davis, A.; Deming, DA.; et al. Treatment of Metastatic Colorectal Cancer: ASCO Guideline. J Clin Oncol. 2023, 41, 678-700.
4. Liu, W.; Yan, XL.; Wang, K.; Bao, Q.; Sun, Y.; Xing, BC. The outcome of liver resection and lymphadenectomy for hilar lymph node involvement in colorectal cancer liver metastases. Int J Colorectal Dis. 2014, 29, 737-45.
5. Elias, D.; Saric, J.; Jaeck, D.; Arnaud, JP.; Gayet, B.; Rivoire, M.; Lorimier, G.; Carles, J.; Lasser, P. Lasser Prospective study of microscopic lymph node involvement of the hepatic pedicle during curative hepatectomy for colorectal metastases. Br J Surg. 1996, 83, 942–5.
6. Ercolani, G.; Grazi, GL.; Ravaioli, M.; Grigioni, WF.; Cescon, M.; Gardini, A.; Del Gaudio, M.; Cavallari, A. The role of lymphadenectomy for liver tumors: further considerations on the appropriateness of treatment strategy. Ann Surg. 2004, 239, 202-9.
7. Shizuka, D.; Shirai, Y.; Hatakeyama, K. Ischemic biliary stricture due to lymph node dissection in the hepatoduodenal ligament. Hepatogastroenterology. 1998, 45, 2048-50.
8. Grobmyer, SR.; Wang, L.; Gonen, M.; Fong, Y.; Klimstra, D.; D'Angelica, M.; DeMatteo, RP.; Schwartz, L.; Blumgart, LH.; Jarnagin, WR. Perihepatic lymph node assessment in patients undergoing partial hepatectomy for malignancy. Ann Surg 2006; 244:260-4.
9. Rau, C.; Blanc, B.; Ronot, M.; Dokmak, S.; Aussilhou, B.; Faivre, S.; Vilgrain, V.; Paradis, V.; Belghiti, J. Neither preoperative computed tomography nor intra-operative examination can predict metastatic lymph node in the hepatic pedicle in patients with colorectal liver metastasis. Ann Surg Oncol. 2012, 19, 163–8.
10. Ko, CC.; Yeh, LR.; Kuo, YT.; Chen, JH. Imaging biomarkers for evaluating tumor response: RECIST and beyond. Biomark Res. 2021, 9, 52.
11. Messina, C.; Bignone, R.; Bruno, A.; Bruno, A.; Bruno, F.; Calandri, M.; Caruso, D.; Coppolino, P.; Robertis, R.; Gentili, F.; et al. Diffusion-Weighted Imaging in Oncology: An Update. Cancers (Basel). 2020, 12, 1493.
12. Bonekamp, S.; Corona-Villalobos, CP.; Kamel, IR. Oncologic applications of diffusion-weighted MRI in the body. J Magn Reson Imaging. 2012, 35, 257-79.
13. Sumi, M.; Sakihama, N.; Sumi, T.; Morikawa, M.; Uetani, M.; Kabasawa, H.; Shigeno, K.; Hayashi, K.; Takahashi, H.; Nakamura, T. Discrimination of metastatic cervical lymph nodes with diffusion-weighted MR imaging in patients with head and neck cancer. AJNR Am J Neuroradiol. 2003, 24, 1627-34.
14. Abdel, Razek, AA.; Soliman, NY.; Elkhamary, S.; Alsharaway, MK.; Tawfik A. Role of diffusion-weighted MR imaging in cervical lymphadenopathy. Eur Radiol. 2006, 16, 1468-77.
15. Eiber, M.; Beer, AJ.; Holzapfel, K.; Tauber, R.; Ganter, C.; Weirich, G.; Krause, BJ.; Rummeny, EJ.; Gaa, J. Preliminary results for characterization of pelvic lymph nodes in patients with prostate cancer by diffusion-weighted MR-imaging. Invest Radiol. 2010, 45, 15-23.
16. Zhou, XJ.; Gao, Q.; Abdullah, O.; Magin, RL. Studies of anomalous diffusion in the human brain using fractional order caculous. Magn Reson Med. 2010, 63, 562–569.
17. Ai, Z.; Han, Q.; Huang, Z.; Wu, J.; Xiang, Z. The value of multiparametric histogram features based on intravoxel incoherent motion diffusion-weighted imaging (IVIM-DWI) for the differential diagnosis of liver lesions. Ann Transl Med. 2020, 8, 1128.
18. Bennett, KM.; Schmainda, KM.; Bennett, RT.; Rowe, DB.; Lu, H.; Hyde, JS. Characterization of continuously distributed cortical water diffusion rates with a stretched-exponential model. Magn Reson Med. 2003, 50, 727–734.
19. Liu, C.; Wang, K.; Li, X.; Zhang, J.; Ding, J.; Spuhler, K.; Duong, T.; Liang, C.; Huang C. Breast lesion characterization using whole-lesion histogram analysis with stretched-exponential diffusion model. J Magn Reson Imaging. 2018, 47, 1701-1710.

20. Seo, N.; Chung, YE.; Park, YN.; Kim, E.; Hwang, J.; Kim, MJ. Liver fibrosis: stretched exponential model outperforms mono-exponential and bi-exponential models of diffusion-weighted MRI. Eur Radiol. 2018, 28, 2812-2822.
21. Bai, Y.; Lin, Y.; Tian, J.; Shi, D.; Cheng, J.; Haacke, EM.; Hong, X.; Ma, B.; Zhou, J.; Wang, M. Grading of gliomas by using monoexponential, biexponential, and stretched exponential diffusion-weighted MR imaging and diffusion kurtosis MR imaging. Radiology. 2016, 278, 496-504.
22. Wang, F.; Wang, Y.; Zhou, Y.; Liu, C.; Xie, L.; Zhou, Z.; Liang, D.; Shen, Y.; Yao, Z.; Liu, J. Comparison between types I and II epithelial ovarian cancer using histogram analysis of monoexponential, biexponential, and stretched-exponential diffusion models. J Magn Reson Imaging. 2017, 46, 1797-1809.
23. Wang, Y.; Hu, D.; Yu, H.; Shen, Y.; Tang, H.; Kamel, IR.; Li, Z. Comparison of the Diagnostic Value of Monoexponential, Biexponential, and Stretched Exponential Diffusion-weighted MRI in Differentiating Tumor Stage and Histological Grade of Bladder Cancer. Acad Radiol. 2019, 26, 239-246.
24. Hu, Y.; Tang, H.; Li, H.; Li, A.; Li, J.; Hu, D.; Li, Z.; Kamel, IR. Assessment of different mathematical models for diffusion-weighted imaging as quantitative biomarkers for differentiating benign from malignant solid hepatic lesions. Cancer Med. 2018, 7, 3501-3509.
25. Li, H.; Liang, L.; Li, A.; Hu, Y.; Hu, D.; Li, Z.; Kamel, IR. Monoexponential, biexponential, and stretched exponential diffusion-weighted imaging models: quantitative biomarkers for differentiating renal clear cell carcinoma and minimal fat angiomyolipoma. J Magn Reson Imaging. 2017, 46, 240-247.
26. Kim, HC.; Seo, N.; Chung, YE.; Park, MS.; Choi, JY.; Kim, MJ. Characterization of focal liver lesions using the stretched exponential model: comparison with monoexponential and biexponential diffusion-weighted magnetic resonance imaging. Eur Radiol. 2019, 29, 5111-5120.
27. Jerome, NP.; Miyazaki, K.; Collins, DJ.; Orton, MR.; d'Arcy, JA.; Wallace, T.; Moreno, L.; Pearson, AD.; Marshall, LV.; Carceller, F; et al. Repeatability of derived parameters from histograms following non-Gaussian diffusion modelling of diffusion-weighted imaging in a paediatric oncological cohort. Eur Radiol. 2017, 27, 345-353.
28. Jia, H.; Jiang, X.; Zhang, K.; Shang, J.; Zhang, Y.; Fang, X.; Gao, F.; Li, N.; Dong, J. A Nomogram of Combining IVIM-DWI and MRI Radiomics From the Primary Lesion of Rectal Adenocarcinoma to Assess Nonenlarged Lymph Node Metastasis Preoperatively. J Magn Reson Imaging 2022; 56:658-667.
29. Wang, C.; Yu, J.; Lu, M.; Li, Y.; Shi, H.; Xu, Q. Diagnostic Efficiency of Diffusion Sequences and a Clinical Nomogram for Detecting Lymph Node Metastases from Rectal Cancer. Acad Radiol. 2022, 29, 1287-1295.
30. Zhu, HB.; Xu, D.; Sun, XF.; Li, XT.; Zhang, XY.; Wang, K.; Xing, BC.; Sun, YS. Prediction of hepatic lymph node metastases based on magnetic resonance imaging before and after preoperative chemotherapy in patients with colorectal liver metastases underwent surgical resection. Cancer Imaging. 2023, 23, 18.